

# Continuous Sensing of Blood by Dark-field Microscopy and Surface-enhanced Raman Spectroscopy

A.-I. Henry<sup>\*</sup>, B. Sharma, and R. P. Van Duyne

Department of Chemistry, Northwestern University, Evanston, IL, USA,

<sup>\*</sup>a-henry@northwestern.edu

## ABSTRACT

Surface-enhanced Raman spectroscopy (SERS) is a rapid, label-free technique with multiplexing capabilities, making it very relevant for the sensitive real-time detection for biomedical applications. We have integrated SERS-active nanoparticles (nanotags) with a microfluidic device for the future detection of biomarkers in blood. We have developed a SERS imaging set-up in order to detect the SERS signal from multiple nanotags at the same time. We also imaged the nanotags by dark-field Rayleigh scattering, and were able to locate those particles in human blood. Finally, we probe the SERS signal of nanotags dispersed in optically clear solution (methanol) and human blood. No significant difference in the SERS intensity was observed.

**Keywords:** nanoparticles, biosensing, imaging, diagnostics, surface-enhanced Raman spectroscopy

## 1 INTRODUCTION

Life-threatening bloodborne infections such as sepsis necessitate an early diagnosis and treatment to increase chances of survival for the patient. The ability to rapidly detect the molecular and pathogenic markers for sepsis requires the development of new sensing technologies with specific requirements: rapid, label-free, with no extended processing of the sample, able to detect multiple targets simultaneously, and sufficiently stable towards fouling to permit continuous sensing over clinically relevant timescales.

Surface-enhanced Raman spectroscopy (SERS) integrates all of these requirements, and has emerged as a very valuable tool for the sensitive real-time detection for biomedical applications<sup>1-3</sup>. As no two molecules have identical Raman spectra, Raman scattering is inherently a label-free technique and capable of discriminating between many potential biological markers such as small molecules, bacteria, and proteins. SERS overcomes the inherent problem of low sensitivity of Raman scattering by amplifying the intensity of the Raman signal by 6 - 9 orders of magnitude by reversibly capturing/partitioning the analytes within ~2 nm of a nanostructured noble metal surface. Demonstration of *in vivo* glucose detection with unprecedented sensitivity (micromolar to picomolar concentration sensitivity) in a rat model has been made recently in our group.<sup>4</sup> The enhancement itself originates

from two enhancing mechanisms, namely the electromagnetic and the chemical enhancement. The latter is reported to have a relatively minor contribution to the overall enhancement. The electromagnetic enhancement is produced when molecules lie in the vicinity of plasmonic (Ag, Au...) substrates that are nanostructured.<sup>5,6</sup> This nanostructuring acts like an antenna, resulting in the extremely high intensity of the Raman scattered light arising from the molecule(s) in the electromagnetic hot spot. Typical SERS substrate are Ag or Au aggregated colloids, Ag or Au pillar-like or rough films.<sup>5</sup> The SERS-active nanoaggregates – or nanotags- used here are more elaborate and robust than normal colloids as the metallic nanoparticles are monodisperse in size and their mechanical and chemical stability is ensured by the silica shell in which they are embedded.

SERS is a relatively newly developed technique for noninvasive preclinical imaging, but presents many advantages. The detection limit of SERS is extremely low as stated previously. Furthermore, the multiplexing capabilities associated with SERS are greatly relevant to the field of molecular imaging.<sup>2,3,7,8</sup>

## 2 MATERIALS AND METHODS

SERS-active nanoparticles were provided by Cabot Security Materials, Inc. (Mountain View, CA). The SERS imaging set-up used in this work was assembled in the lab. Components include: an inverted microscope (Nikon Ti-U/E20L80) equipped with a 20X air objective, a galvo-scanner (Thorlabs, Inc., New Jersey), a 0.5 m imaging spectrograph (Acton-2556, Princeton Instruments, New Jersey), and an electron multiplying CCD camera (ProEM 1600, Princeton Instruments, New Jersey).

Whole human blood was purchased from BioChemEd Services (Winchester, VA), stored in a fridge between 2 and 5 °C and used within three weeks from the draw date. The blood was allowed to warm up at room temperature for ~ 5 min. before experiments were started.

## 3 EXPERIMENTAL RESULTS

### 3.1 SERS imaging of nanotags

The SERS-active nanoparticle aggregates used in this work consist of Au-silica core-shell nanoparticles with Raman target analytes adsorbed at the interface. Details on

the synthesis and assembly of the nanotags can be found elsewhere<sup>9</sup>. The number of cores within a nanotag (encased in a single silica shell) may vary from one (monomer) to twelve (dodecamer) or more, with an average diameter of 96 +/- 11nm in diameter<sup>10</sup>. The average silica shell thickness is 63 +/- 4 nm. Monomers are of very limited interest though since they contribute very little ( $< 10^3$ ) to the SERS signal compared to nanotags with at least two cores, i.e. that have an electromagnetic hot spot allowing to reach high enhancements ( $\sim 10^8$ ). A schematic of a dimer nanotag is presented in Figure 1A. The organic molecule used as Raman target analyte was 1,2-bis(4-pyridyl)ethylene (BPE). This molecule is a well-known non-resonant Raman scatterer providing relatively large enhancements and routinely used in the laboratory.<sup>11</sup>

Nanotags dispersed in water were drop-cast ( $\sim 10 \mu\text{L}$ ) on a clean microscope glass slide and allowed to sit at room temperature while the solvent evaporated. The SERS imaging was performed at a 785 nm excitation wavelength on the nanotags immobilized on the glass slides. In Figure 1B, a color image of an area covered with such nanotags is presented. The probed area, i.e. the field of view, is about  $\sim 20 \times 20 \mu\text{m}$  wide. The SERS enhancing areas appear as colored spots on a black background. The SERS intensity scale goes from black (no SERS activity) to white (highest SERS intensity) while the blue dots represent areas of moderate to high SERS enhancement, which likely corresponds to nanotags. The white dots within the blue areas clearly indicate the presence of electromagnetic hot spot(s), which is consistent with the Au cores aggregated structures of the nanotags. It would be possible to elucidate the structure of the nanotags probed and present on the SERS image by performing a structure-property correlated experiment on the same sample, using a marked substrate that is compatible with scanning or transmission electron microscopy.<sup>12</sup> The surface-enhanced Raman (SER) spectra can be extracted from the SERS image by 'slices', as shown in Figure 1C. The spectrum presented in Figure 1C shows all the features expected on the Raman or SER spectrum of BPE, which is the target analyte. Note that the signal to noise ratio of the spectrum is very good and compared well to the one of a spectrum taken on a regular non-imaging set-up. Overall, the SERS imaging capability allows to upscale the probing of the SERS activity to a 2D sample, which increases the productivity for SERS detection of nanoprobe without compromising the sensitivity. Ultimately, this technique is of great use for multiple applications, such as real-time monitoring of SERS-active probes in a given environment.

### 3.2 Nanotags detection through blood

The nanotags described above present multiple advantages when it comes to use them as detection probes. For example, they can be used for indirect detection of biological molecules when appropriately functionalized with antigens. The silica shell is indeed an excellent surface

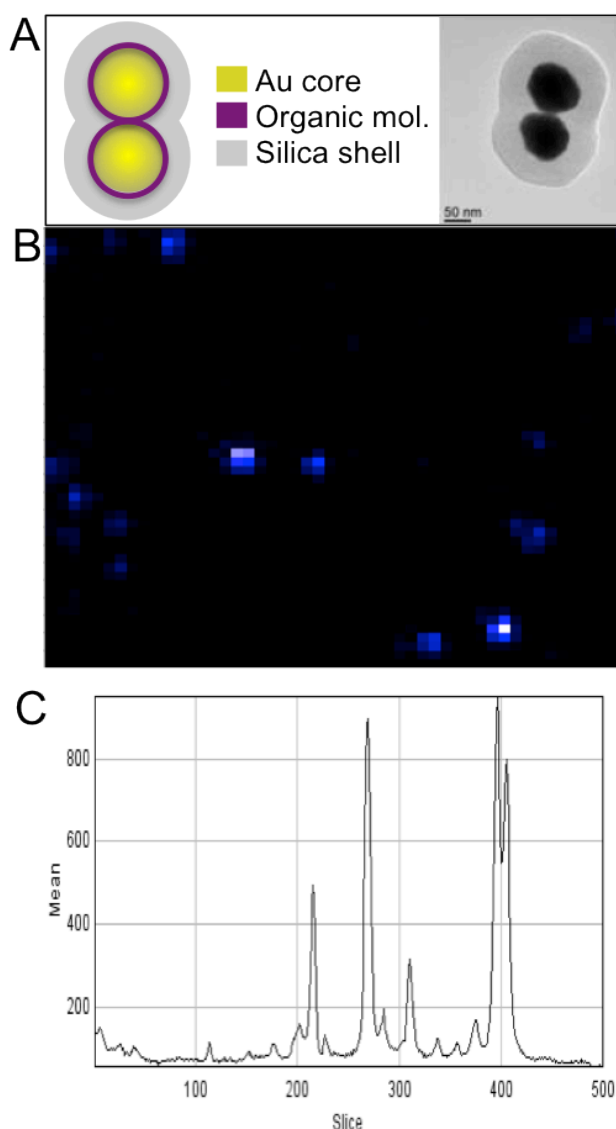


Figure 1. SERS imaging of SERS-active nanoparticles. A: sketch of the nanotags made of Au cores and  $\text{SiO}_2$  shells between which organic molecules are embedded ; a TEM image of a dimer is shown on the right. B: SERS image of nanotags immobilized on glass. of nanotags at 785 nm excitation wavelength. The blue dots are the SERS-active nanotags. The white dots represent the highest intensity areas (electromagnetic hot spots). C: SER spectrum of the reporter molecule (here, BPE).

for biomolecule attachment, either by direct, covalent attachment, or by indirect means.<sup>13</sup> Furthermore, SERS detection provides invaluable information on multiple target analytes (biomarkers, ligands...) as the molecular vibrational features are unique and act as fingerprint-like signatures. This very unique characteristic allows for performing multiplexed experiments with one single measurement, even in tissue in a living rat.<sup>3</sup> Motivated by the need to extent the detection of nanotags to another

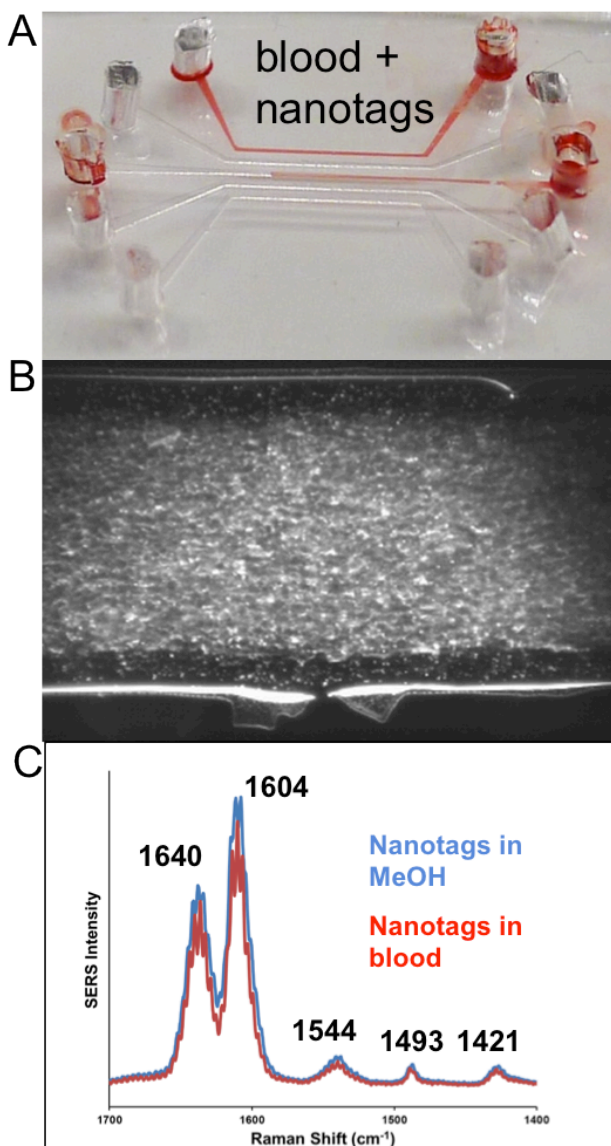


Figure 2. Detection of SERS-active nanoparticles through human blood. A. photograph of a 5 channel-microfluidic device, whose top channel has been filled in with human blood and nanotags. B. Dark-field Rayleigh scattering image of the channel in A, where the white dots are the nanotags and the middle region is blood, with red blood cells visible. C. SER spectra of nanotags in methanol (blue trace) and blood (red trace) showing no significant decrease in the scattered intensity

biological compartment for the detection of pathogens, we have monitored nanotags by SERS in whole human blood.

In order to probe for continuous SERS sensing in flowing blood, we have used a microfluidic device. This device consists of a 5-channel polydimethylsiloxane (PDMS) device sealed on top of an ultrathin glass slide. The optical transparency of the glass allows for working in transmission and collecting light from the device for micro-

and spectroscopy.

A photograph of the device is presented in Figure 2A. Nanotags in solution in methanol are injected in a channel with a micropipette ( $\sim 10 \mu\text{L}$ ). Blood is later injected in the same channel using the same method. In order to ensure nanotags and blood were mixed within the channel, we perform dark-field optical microscopy on the sample, as shown in Figure 2B. The small metallic core of the nanotags make them extremely good candidates for this technique, as they scatter light (Rayleigh scattering) extremely well and appear in Figure 2B as the small white dots between the two horizontal lines (edges of the microfluidic channel). On the same image, the gray matter in the middle of the channel is the blood; biconcave red blood cells can be observed. From Figure 2B, it is clear that nanotags and blood mix within the microfluidic channel.

SERS measurements on nanotags in the microfluidic channel are performed before and after blood injection. The two SER spectra are presented in Figure 2C, where the blue trace corresponds to the nanotags in methanol (before blood injection) and the red trace to the nanotags in blood. As seen in Figure 2C, both spectra present the multiple characteristic Raman peaks of BPE (labeled).

Two important results are obtained from this experiment. First, no interaction from the PDMS edges of the channel is observed. Second, no significant absorption of the scattered light by the blood is observed; the SERS intensity collected through blood is about the same as the one in methanol.

## 4 CONCLUSION

We report the detection of SERS-active nanoprobe – nanotags- by a SERS imaging set-up in air and by dark-field Rayleigh scattering and SERS through blood in a microfluidic device.

To our knowledge, this report is the first evidence that nanotags can be detected through blood with no significant decrease in the collected SERS intensity.

## 5 ACKNOWLEDGMENTS

We thank Drs. R. Griffith Freeman and Michael J. Natan from Cabot Security Materials, Inc for providing us with the nanotags. We thank Dr. Laura B. Sagle from Northwestern University for fabricating the microfluidic device. This work supported by DARPA under SSC Pacific grant N66001-11-1-4179. Any opinions, findings, and conclusions or recommendations expressed in this publication are those of the author(s) and do not necessarily reflect the views of DARPA.

## 6 REFERENCES

- (1) Kneipp, J.; Kneipp, H.; Kneipp, K. *Chem. Soc. Rev.* **2008**, *37*, 1052.

- (2) Schlücker, S. *ChemPhysChem* **2009**, *10*, 1344.
- (3) Zavaleta, C. L.; Smith, B. R.; Walton, I.; Doering, W.; Davis, G.; Shojaei, B.; Natan, M. J.; Gambhir, S. S. *Proc. Natl. Acad. Sci. U.S.A.* **2009**, *106*, 13511.
- (4) Ma, K.; Yuen, J. M.; Shah, N. C.; Walsh, J. T.; Glucksberg, M. R.; Van Duyne, R. P. *Anal. Chem.* **2011**, *83*, 9146.
- (5) Sharma, B.; Frontiera, R. R.; Henry, A.-I.; Ringe, E.; Van Duyne, R. P. In *Mater. Today*; Elsevier: 2012; Vol. 15, p 16.
- (6) McMahon, J. M.; Li, S.; Ausman, L. K.; Schatz, G. C. *J. Phys. Chem. C* **2011**, *116*, 1627.
- (7) Keren, S.; Zavaleta, C.; Cheng, Z.; de la Zerda, A.; Gheysens, O.; Gambhir, S. S. *Proc. Natl. Acad. Sci. U.S.A.* **2008**, *105*, 5844.
- (8) Qian, X. M.; Nie, S. M. *Chem. Soc. Rev.* **2008**, *37*, 912.
- (9) Wustholz, K. L.; Henry, A.-I.; McMahon, J. M.; Freeman, R. G.; Valley, N.; Piotti, M. E.; Natan, M. J.; Schatz, G. C.; Duyne, R. P. V. *J. Am. Chem. Soc.* **2010**, *132*, 10903.
- (10) Tyler, T. P.; Henry, A.-I.; Van Duyne, R. P.; Hersam, M. C. *J. Phys. Chem. Lett.* **2011**, *2*, 218.
- (11) Yang, W.-h.; Hulteen, J.; Schatz, G. C.; Van Duyne, R. P. *J. Chem. Phys.* **1996**, *104*, 4313.
- (12) Henry, A.-I.; Bingham, J. M.; Ringe, E.; Marks, L. D.; Schatz, G. C.; Van Duyne, R. P. *J. Phys. Chem. C* **2011**, *115*, 9291.
- (13) Doering, W. E.; Piotti, M. E.; Natan, M. J.; Freeman, R. G. *Adv. Mater.* **2007**, *19*, 3100.